THE JOURNAL OF PHYSICAL CHEMISTRY Letters

Letter

pubs.acs.org/JPCL

# Observation of Rhenium Anion and Electron Affinity of Re

Xiaolin Chen[†] and Chuangang Ning*[,†,‡]

[†]Department of Physics, State Key Laboratory of Low-Dimensional Quantum Physics, Tsinghua University, Beijing 100084, China
[‡]Collaborative Innovation Center of Quantum Matter, Beijing 100084, China

**ABSTRACT:** It was believed that the rhenium anion $Re^-$ was not stable, just like $Mn^-$. We report the observation of $Re^-$ in the laser ablation ion source and the further confirmation via the high-resolution photoelectron spectra of $Re^-$. The ground state of $Re^-$ ions is $5d^6 6s^2\ ^5D_4$. The electron affinity of rhenium is determined to be 487.13(51) $cm^{-1}$ or 60.396(63) meV.

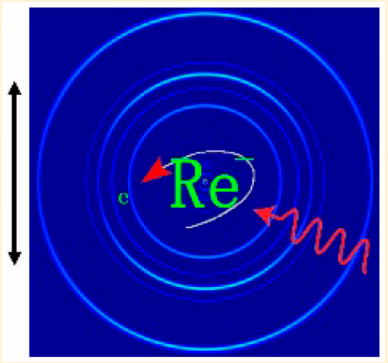


The complex nature of the negative ions of transition elements is noticeable along the Mn, Tc, and Re sequence in the VIIB group. The electronic configuration of the neutral VIIB atoms in the ground state is $nd^5(n+1)s^2$, with $n$ being 3−5. The half-filled d-sub shell and full-filled s-sub shell make their neutral atoms not easily accept electrons to form negative ions. It is well established that a stable $Mn^-$ ion cannot be formed.[1−3] For the homologous 4d (Tc) and 5d (Re) elements, it is still unclear whether the elements can form stable negative ions. The semiempirical method for the electron affinity (EA) values of transition elements predicted that both EA values of Mn and Tc were close to 1 eV, whereas the EA of Re was ∼1.6 eV.[3] However, O'Malley and Beck predicted that the $Re^-$ ($5d^6 6s^2\ ^5D_4$) level is slightly unbound (on the order of 10 meV) by the high-level relativistic configuration-interaction calculations. Similar calculations for the binding energies of the $Tc^-(4d^6 5s^2\ ^5D_J)$ levels suggest that the binding energy values range from 636 meV for $J = 4$ to 460 meV for $J = 0$, whereas the calculations confirm that the $Mn^-$ ion should be unbound by >1 eV. Recently, Wu et al. predicted the EA of Re to be 0.017, −3.936, and −3.950 eV using the theoretical B3LYP, CCSD(T), and MP2 methods, respectively.[4] Scheer et al. reported the measured EA values of Re as 0.15(10) eV via the self-surface ionization method.[5] However, the self-surface ionization method cannot provide unambiguous evidence of the existence of stable $Re^-$. The mass spectroscopy cannot exclude the possibility of an isobar contamination due to the same mass number of other species. This was the status for Re when the newest review of binding energies for atomic ions appeared in 2004.[6] It was still an open question whether $Re^-$ and $Tc^-$ were stable before the present work. The radioactivity of Tc adds an extra challenge to measure its EA. In this work, we report the observation of $Re^-$ and the high-resolution photoelectron spectroscopy of $Re^-$. The spectroscopic data provide the unambiguous evidence of the existence of stable $Re^-$ ions.

Negative ions themselves are a unique species. Their electronic structures are intrinsically different from those of neutral atoms or positive ions.[7] The electron affinity (EA) is one of the fundamental parameters of an atom. The measured accuracy of EAs of atoms has steadily improved over the past almost 50 years.[2,8,9] However, the uncertainty of EAs for many transition elements still remains ∼10 meV due to the low cross-section of p-wave threshold photodetachment and the complicated electronic structures of transition elements.[2] Recently, our group has significantly improved the accuracy of EA values for transition metals via the slow-electron velocity-map imaging (SEVI) method.[10−16] For example, the electron affinity of Nb was measured as 0.91740(6) eV via SEVI method, which has been improved by a factor of >400 with respect to the previous work.[17] The accurate experimental EA value of Re measured in the present work could serve as a benchmark for developing more accurate theoretical methods for $Re^-$.

Our experiment was carried out using a high-resolution photoelectron imaging apparatus. Its details have been previously described.[12] In brief, the apparatus consists of a laser ablation ion source, a Wiley−McLaren-type time-of-flight (TOF) mass spectrometer, and a photoelectron velocity-map imaging system.[18] The rhenium negative ions were produced by the pulsed laser ablation ion source operated at 20 Hz repetition rate. The 532 nm light from a pulsed Nd:YAG laser (∼10 mJ/pulse) was focused onto a rotating and translating rhenium metal disk. The ions were extracted and accelerated in a time-of-flight (TOF) mass spectrometer. The $Re^-$ ions were

**Received:** May 4, 2017
**Accepted:** June 5, 2017
**Published:** June 5, 2017





DOI: 10.1021/acs.jpclett.7b01079
J. Phys. Chem. Lett. 2017, 8, 2735−2738

selected by a mass gate and then were photodetached by a tunable dye laser in the interaction region of the velocity-map imaging system. The outgoing photoelectrons were projected onto a phosphor screen enhanced by a set of microchannel plates and recorded by a CCD camera. The polarization vector of the linearly polarized dye laser beam is parallel to the screen. The distribution of the projected photoelectrons has a cylindrical symmetry respect to the polarization. As a result, the 3D photoelectron distribution can be reconstructed from the projected 2D image. In the present work, the reconstruction was done by the maximum-entropy method.[19] The imaging voltage −650 V is used for the full energy spectrum measurement. It is −150 V for the electron affinity measurement. The energy resolution is 3.3 $cm^{-1}$ for the kinetic energy $E_k$ 25 $cm^{-1}$, which is a typical $E_k$ for the present EA measurement.

In addition to the photoelectron energy spectrum, the photoelectron angular distribution (PAD) can also be obtained from the photoelectron imaging technique. For a one photon detachment with linearly polarized light, PAD can be described by the formula[20]

$$\frac{d\sigma}{d\Omega} = \frac{\sigma_{total}}{4\pi}\left(1 + \beta\left(\frac{3}{2}\cos^2\theta - \frac{1}{2}\right)\right)$$

Here $\theta$ is the outgoing direction of the photoelectron relative to the polarization axis of the laser and $\sigma_{total}$ is the total photodetachment cross section. $\beta$ is the asymmetry parameter. It ranges between $-1 \le \beta \le 2$. For a given transition, the value of $\beta$ depends on the kinetic energy of photoelectrons.

Figure 1 shows the mass spectrum of anions produced via the laser ablation of a pure rhenium metal disk. The natural

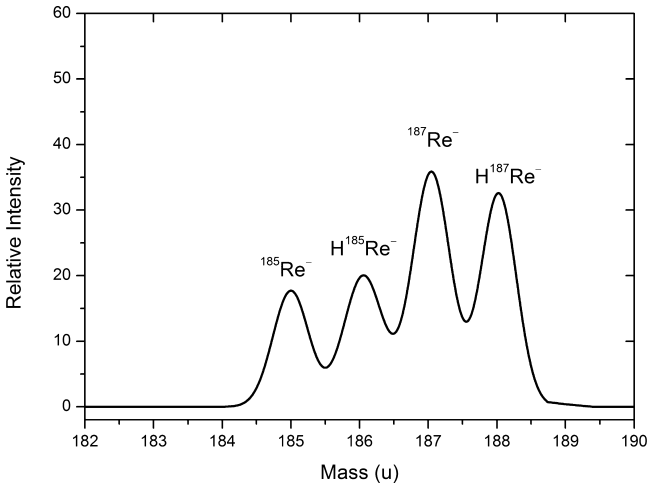


**Figure 1.** Mass spectrum of rhenium and rhenium hydride anions produced via the laser ablation source.

abundances of the isotopes of rhenium are $^{185}$Re 37.40% and $^{187}$Re 62.60%, respectively. The four mass peaks in Figure 1 can be assigned as $^{185}Re^-$, $H^{185}Re^-$, $^{187}Re^-$, and $H^{187}Re^-$. The $^{187}Re^-$ peak was selected for measuring the electron affinity of Re. The selected peak may contain a small amount of $H_2{}^{185}Re^-$ due to the same mass number. The contribution of $H_2{}^{185}Re^-$ should be <5% via the analysis of the intensity ratios according to the natural isotope abundance.

As shown in Figure 2, the energy spectrum of $Re^-$ measured at the photon energy $h\nu$ = 16387.35 $cm^{-1}$ has five well-resolved

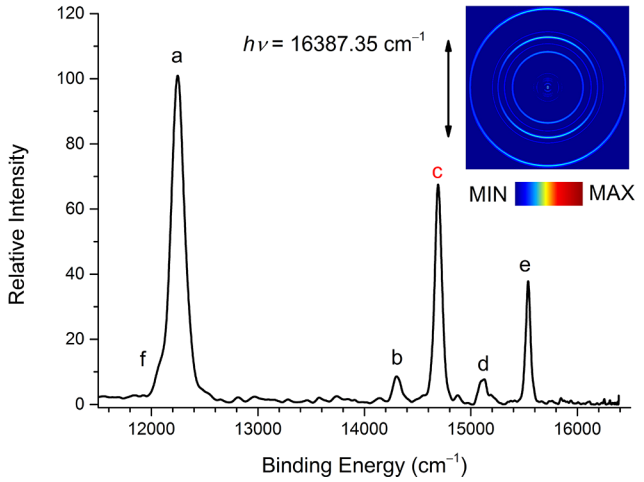


**Figure 2.** Photoelectron spectrum of $Re^-$ at the photon energy of 16 387.35 $cm^{-1}$. The inset shows the photoelectron imaging. The double arrow indicates the laser polarization. Peak c is related to the transition $Re(^6D_{7/2}) \leftarrow Re^-(^5D_4)$, which is used to measure the electron affinity of Re.

peaks under the imaging voltage −650 V. These peaks are related to six transitions, which are labeled as a−f. Peak f is relatively weak, and appears as a shoulder of peak a. All related

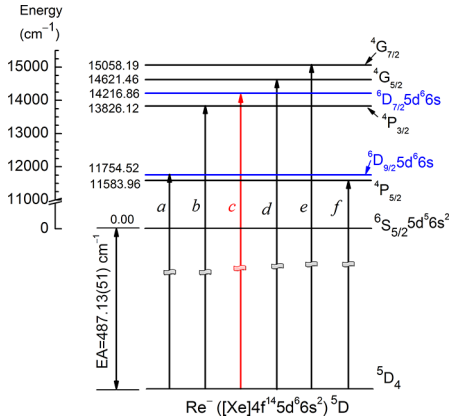


**Figure 3.** Energy levels of Re related to the present measurement. The ground state of Re is $^6S_{5/2}$.The ground state of $Re^-$ is $^5D_4$. The electronic configurations of the final states of transitions a and c are $5d^6$ 6s, which were plotted as blue lines, while the configuration of the other states is $5d^5$ $6s^2$ plotted as black lines.

transitions are illustrated in Figure 3. The ground state of Re is $^6S_{5/2}$ ($5d^56s^2$), and the ground state of $Re^-$ is $^5D_4$ ($5d^66s^2$). The six transitions are from the common ground state of $Re^-$ to the six different neutral states of Re. The accurate data of the energy levels of neutral Re atoms are well known,[21] which can be taken as the fingerprints for the assignment. The peaks a and c are results of photodetachment of a 6s electron. The photoelectron detached from an s subshell produces a p wave, which has a theoretical $\beta$ value of 2. The observed $\beta$ values of peaks a and c are 1.3 and 1.7, respectively. The peaks b, d, e, and f are results of the photodetachment from a 6d electron. The photoelectron angular distributions are the mixed results of the p partial wave and the f partial wave. Their $\beta$ values depend on the kinetic energy of photoelectrons.[22] It should be noted that the other open channels may have non-negligible influence



DOI: 10.1021/acs.jpclett.7b01079
J. Phys. Chem. Lett. 2017, 8, 2735−2738

on the measured $\beta$ values, especially for those weak peaks, because of the overlapped projections. The measured results were summarized in Table 1. Because the transition energy

**Table 1. Peak Positions, Assignments for the $Re^-$ SEVI Spectra, the Asymmetry Parameter $\beta$ at the Photon Energy of 16 387.35 $cm^{-1}$, and the Electron Affinity of Re**

| peak | levels (Re ← $Re^-$) | binding energy ($cm^{-1}$) | $\beta$ value |
|---|---|---|---|
| *a* | $^6D_{9/2} \leftarrow {}^5D_4$ | 12249.9(9.0) | 1.3 |
| *b* | $^4P_{3/2} \leftarrow {}^5D_4$ | 14308.0(8.2) | 0.2 |
| *c* | **$^6D_{7/2} \leftarrow {}^5D_4$** | **14703.99(51)** | **1.7** |
| *d* | $^4G_{5/2} \leftarrow {}^5D_4$ | 15114.9(9.0) | 0.1 |
| *e* | $^4G_{7/2} \leftarrow {}^5D_4$ | 15538.2(8.0) | 0.6 |
| *f* | $^4P_{5/2} \leftarrow {}^5D_4$ | 12071.09[a] | |
| electron affinity | 487.13(51) $cm^{-1}$ or 60.396(63) meV | | |

[a]It is a calculated value according to the binding energy of peak *c* and the energy gap between $^6D_{7/2}$ and $^4P_{5/2}$.

from the anion ground state $Re^-(^5D_4)$ to the ground neutral state $Re(^6S_{5/2})$ is out of the tuning range of our dye laser system and the neutral Re atomic energy levels are well known with a high accuracy, the relatively stronger transition *c* [$Re(^6D_{7/2}) \leftarrow Re^-(^5D_4)$] is selected as the target channel for the present EA measurement.

A primary measurement of the binding energy of the transition c can help us to narrow down the range for performing a series of low-kinetic-energy photoelectron measurement to achieve a high accuracy of EA value. A series of photoelectron spectra were measured with the photon energy scanned from 14 720 to 14 740 $cm^{-1}$ with a step 5 $cm^{-1}$ at the imaging voltage −150 V. Hence the kinetic energy $E_k$ for channel c varied from 15 to 35 $cm^{-1}$. Figure 4 shows the

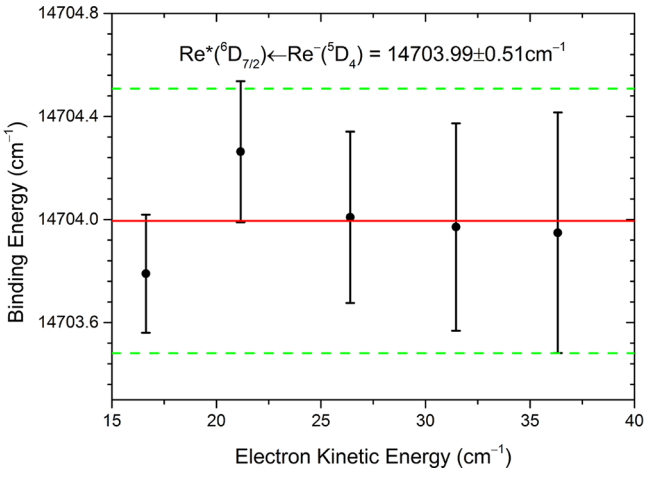


**Figure 4.** Binding energy of $Re(^6D_{7/2}) \leftarrow Re^-(^5D_4)$ transition measured as a function of the photoelectron kinetic energy. The dotted lines indicate the ±0.51 $cm^{-1}$ uncertainty.

binding energy of transition c measured at the different kinetic energy $E_k$. The mean binding energy of peak c is 14 703.99 $cm^{-1}$ with an uncertainty 0.51 $cm^{-1}$. The uncertainty 0.51 $cm^{-1}$ has included the contribution of the laser line width 0.06 $cm^{-1}$. By subtracting the energy 14 216.86 $cm^{-1}$ of Re $(^6D_{7/2})$,[21] the electron affinity of Re is determined to be 487.13(51) $cm^{-1}$ or 60.396(63) meV. This is the lowest reported EA value among the transition elements that can form stable negative ions. The accurate experimental EA value determined in the present work could serve as a benchmark for developing more accurate theoretical methods for transition metals.

The stable negative rhenium anions were produced via the laser ablation ion source. The high-resolution photoelectron spectra provided an unambiguously confirmation of stable Re anions. The electron affinity Re was determined to be 487.13(51) $cm^{-1}$ or 60.396(63) meV. The value determined in this study could serve as a benchmark for developing theoretical methods for transition metals, especially in VII B group.

## AUTHOR INFORMATION


### Corresponding Author

*E-mail: ningcg@tsinghua.edu.cn.

### ORCID

Chuangang Ning: 0000-0002-3158-1253


### Notes

The authors declare no competing financial interest.

## ACKNOWLEDGMENTS

This work is supported by National Natural Science Foundation of China (NSFC) (Grant No. 91336104).

## REFERENCES


(1) Hotop, H.; Lineberger, W. C. Binding Energies in Atomic Negative Ions. *J. Phys. Chem. Ref. Data* **1975**, *4*, 539−576.

(2) Hotop, H.; Lineberger, W. C. Binding Energies in Atomic Negative Ions:II. *J. Phys. Chem. Ref. Data* **1985**, *14*, 731−750.

(3) O'Malley, S.; Beck, D. R. Binding Energies of $4d^6 5s^2$ States in $Tc^-$. *Phys. Rev. A* **2002**, *65*, 064502.

(4) Wu, Z. J.; Kawazoe, Y. Electron Affinities and Ionization Potential of 4d and 5d Transition Metals by CCSD(T), MP2 and Density Functional Theory. *Chem. Phys. Lett.* **2006**, *423*, 81−86.

(5) Scheer, M. D.; Fine, J. Positive and Negative Self-Surface Ionization of Tungsten and Rhenium. *J. Chem. Phys.* **1967**, *46*, 3998−4003.

(6) Andersen, T. Atomic Negative Ions: Structure, Dynamics and Collisions. *Phys. Rep.* **2004**, *394*, 157−313.

(7) Rienstra-Kiracofe, J. C.; Tschumper, G. S.; Schaefer, H. F., III; Nandi, S.; Ellison, G. B. Atomic and Molecular Electron Affinities: Photoelectron Experiments and Theoretical Computations. *Chem. Rev.* **2002**, *102*, 231−282.

(8) Lineberger, W. C. Once upon Anion: A Tale of Photodetachment. *Annu. Rev. Phys. Chem.* **2013**, *64*, 21−36.

(9) Lineberger, W. C.; Woodward, B. W. High Resolution Photodetachment of S− Near Threshold. *Phys. Rev. Lett.* **1970**, *25*, 424−427.

(10) Luo, Z. H.; Chen, X. L.; Li, J. M.; Ning, C. G. Precision Measurement of the Electron Affinity of Niobium. *Phys. Rev. A* **2016**, *93*, 020501.

(11) Chen, X. L.; Luo, Z. H.; Li, J. M.; Ning, C. G. Accurate Electron Affinity of Iron and Fine Structure of Negative Iron Ions. *Sci. Rep.* **2016**, *6*, 24996.

(12) Chen, X. L.; Ning, C. G. Accurate Electron Affinity of Co and Fine-Structure Splitting of $Co^-$ via Slow-Electron Velocity-Map Imaging. *Phys. Rev. A* **2016**, *93*, 052508.

(13) Fu, X.; Luo, Z. H.; Chen, X. L.; Li, J. M.; Ning, C. G. Accurate Electron Affinity of V and Fine-Structure Splitting of $V^-$ via Slow-Electron Velocity-Map Imaging. *J. Chem. Phys.* **2016**, *145*, 164307.

(14) Osterwalder, A.; Nee, M. J.; Zhou, J.; Neumark, D. M. High Resolution Photodetachment Spectroscopy of Negative ions via Slow Photoelectron Imaging. *J. Chem. Phys.* **2004**, *121*, 6317−6322.

(15) Neumark, D. M. Slow Electron Velocity-Map Imaging of Negative Ions: Application to Spectroscopy and Dynamics. *J. Phys. Chem. A* **2008**, *112*, 13287−13301.




DOI: 10.1021/acs.jpclett.7b01079
*J. Phys. Chem. Lett.* 2017, 8, 2735−2738

(16) Leon, I.; Yang, Z.; Liu, H. T.; Wang, L. S. The Design and Construction of a High-Resolution Velocity Imaging Apparatus for Photoelectron Spectroscopy Studies of Sized-Selected Clusters. *Rev. Sci. Instrum.* **2014**, *85*, 083106.
(17) Feigerle, C. S.; Corderman, R. R.; Bobashev, S. V.; Lineberger, W. C. Binding Energies and Structure of Transition Metal Negative Ions. *J. Chem. Phys.* **1981**, *74*, 1580−1598.
(18) Eppink, A. T. J. B.; Parker, D. H. Velocity Map Imaging of Ions and Electrons using Electrostatic Lenses: Application in Photoelectron and Photofragment Ion Imaging of Molecular Oxygen. *Rev. Sci. Instrum.* **1997**, *68*, 3477−3484.
(19) Dick, B. Inverting Ion Images without Abel Inversion: Maximum Entropy Reconstruction of Velocity Maps. *Phys. Chem. Chem. Phys.* **2014**, *16*, 570−580.
(20) Cooper, J.; Zare, R. N. Angular Distribution of Photoelectrons. *J. Chem. Phys.* **1968**, *48*, 942−943.
(21) Sansonetti, J. E.; Martin, W. C. Handbook of Basic Atomic Spectroscopic Data. *J. Phys. Chem. Ref. Data* **2005**, *34*, 1559−2259 or NIST Atomic Spectra Database version 5.0, 2012, http://www.nist.gov/pml/data/asd.cfm.
(22) Liu, Y.; Ning, C. G. Calculation of Photodetachment Cross Sections and Photoelectron Angular Distributions of Negative Ions Using Density Functional Fheory. *J. Chem. Phys.* **2015**, *143*, 144310.



DOI: 10.1021/acs.jpclett.7b01079
*J. Phys. Chem. Lett.* 2017, 8, 2735−2738